



An implicit scheme for time-fractional coupled generalized Burgers' equation

J. Vigo-Aguiar¹ · Reetika Chawla² · Devendra Kumar² · Tapas Mazumdar²

Received: 23 October 2023 / Accepted: 25 November 2023 / Published online: 6 January 2024
© The Author(s), under exclusive licence to Springer Nature Switzerland AG 2024

Abstract

This article presents an efficient implicit spline-based numerical technique to solve the time-fractional generalized coupled Burgers' equation. The time-fractional derivative is considered in the Caputo sense. The time discretization of the fractional derivative is discussed using the quadrature formula. The quasilinearization process is used to linearize this non-linear problem. In this work, the formulation of the numerical scheme is broadly discussed using cubic B-spline functions. The stability of the proposed method is proved theoretically through Von-Neumann analysis. The reliability and efficiency are demonstrated by numerical experiments that validate theoretical results via tables and plots.

Keywords Generalized time-fractional coupled Burgers' equation · Caputo derivative · Quasilinearization · Implicit scheme · Spline · Stability

Mathematics Subject Classification 26A33 · 65M12 · 35R11 · 41A15 · 65D07

1 Introduction

In recent times, fractional partial differential equations (FPDEs) have played a vital role in the study of various complex processes, they have wide applications in applied sciences and engineering [1–4]. The FPDEs can model natural phenomena better than integer order partial differential equations because fractional

✉ Reetika Chawla
reetika.chawla285@gmail.com

J. Vigo-Aguiar
jvigo@usal.es

Devendra Kumar
dkumar@pilani.bits-pilani.ac.in

¹ Department of Applied Mathematics, University of Salamanca, 37008 Salamanca, Spain

² Department of Mathematics, Birla Institute of Technology and Science, Pilani, Rajasthan 333031, India

derivatives have the non-local property, also termed memory. It is challenging to find the analytical solutions to FPDEs; therefore, researchers have paid attention to developing numerical methods that can evaluate the approximate solutions. Moreover, numerical schemes help to analyze the behavior of PDEs used in various models. Numerous methods have been developed to solve FPDEs, such as the adomian decomposition method [5], radial basis functions (RBFs) approximation method [6], finite difference method [7, 8], variational iteration method [9].

The non-linear models are widely studied to deal with natural phenomena. The first non-linear model that explains the theory of turbulence and shock waves was introduced by Burger [10] in 1948. Benton and Platzman [11] estimated the analytical solution of the Burgers' equation. Since one can obtain the analytical solution to this equation only under certain restricted conditions, several numerical techniques were developed to evaluate this problem's solution. Some of the numerical methods are the compact finite difference method [12], variational method [13], weighted average differential quadrature method [14], local radial basis function method [15], Haar wavelet method [16], etc. Fractional differential equations enhance comprehension of the investigated process. Due to its applications in the approximation theory of flow through a shock wave flowing in a viscous fluid and the Burgers' model of turbulence, finding the approximate analytical solution of the time-fractional Burgers' equation (TFBE) is crucial. Several numerical methods have been studied to solve TFBE, such as finite difference method [17], parametric spline function method [18], finite element method [19], and so on.

The problem of coupled Burgers' equation examining the model of polydisperse sedimentation was first demonstrated by Esipov [20]. This model discusses the evolution of two types of particles' scaled volume concentrations. Many numerical methods have been developed to solve coupled linear/non-linear problems, such as meshfree interpolation method [21], homotopy analysis method [22], cubic B-spline method [23], compact operator method [24], and haar wavelet method [25]. For the study of memory and hereditary properties, fractional system of coupled system of Burgers' equation is considered. Chen and An [26] presented the adomian decomposition method to obtain the numerical solution of coupled Burgers' equation with space and time fractional derivatives. Later, Liu and Hou [27] discussed the generalized differential transform method, which constructs an analytical solution of space and time fractional coupled Burgers' equation. Recently, Mittal and Balyan [28] developed the Chebyshev pseudospectral method to solve this equation. Readers may also refer to the articles that include other numerical methods such as meshfree spectral method [29], Laplace homotopy perturbation method [30], Jacobi spectral collocation method [31].

B-splines are a collection of unique spline functions that can build piece-wise polynomials by determining the proper linear combination. The computational advantage of these functions derives from the fact that every B-spline basis function of order m is nonzero over a maximum of m adjacent intervals and zero otherwise. B-spline basis functions are superior to other basis functions due to their smoothness and capacity to manage local phenomena. Numerous physical models have already been solved using cubic B-spline functions as the basis functions. Burgers' equation was solved by Mittal and Jain [32] using a modified cubic B-spline collocation

approach. In this work, we develop an implicit scheme using cubic B-spline functions for time fractional coupled generalized viscous Burgers' equation. At the initial stage, the problem is discretized using the form of quasilinearization applied on generalized non-linear terms $u^p u_x$ and $v^p v_x$. Then the spline functions are used on the linearized form of the problem to obtain the complete numerical scheme of coupled equations.

This article is organized as follows. In Sect. 2, the discretization process is demonstrated by dividing it into three subsections that explain briefly the discretization of time-fractional derivative, the methodology, and the problem discretization. Further, in Sect. 3, the formulation of the numerical scheme is discussed. In Sect. 4, the stability of the proposed numerical scheme is proved by following the method of Von-Neumann stability analysis. The numerical test examples are presented in Sect. 5, and the tables and plots verify our theoretical results. At last, the conclusions and some references are given.

1.1 Relevance of the work

This work presents an implicit scheme based on the spline technique for fractional coupled Burger equations. In our problem, we have linearized the generalized non-linear terms using linearization technique called quasilinearization that are not explored for this coupled problem. Moreover, we have shown the numerical results that presented the correct orders of convergence in both time and space directions that are not displayed or demonstrated in all published work regarding this problem discussed in the literature.

1.2 Problem statement

The time-fractional coupled generalized Burgers' equation is given by

$$D_t^{\alpha_1} u = u_{xx} + \kappa u^p u_x - \rho_1 (uv)_x + f(x, t), \quad (x, t) \in \Omega_x \times \Omega_t, \quad (1.1a)$$

$$D_t^{\alpha_2} v = v_{xx} + \kappa v^p v_x - \rho_2 (uv)_x + g(x, t), \quad (x, t) \in \Omega_x \times \Omega_t, \quad (1.1b)$$

with the initial conditions

$$u(x, 0) = \phi_1(x), \quad v(x, 0) = \phi_2(x), \quad x \in \overline{\Omega_x}, \quad (1.1c)$$

and the boundary conditions

$$u(a, t) = \psi_1(t), \quad v(a, t) = \psi_2(t), \quad u(b, t) = \varphi_1(t), \quad v(b, t) = \varphi_2(t), \quad t \in \overline{\Omega_t}, \quad (1.1d)$$

where $\Omega_x = (a, b)$, $\Omega_t = (0, T)$, α_1, α_2 lie between 0 and 1; $\kappa, p, \rho_1, \rho_2$ are positive integers; $f(x, t), g(x, t), \phi_1(x), \phi_2(x), \psi_1(t), \psi_2(t), \varphi_1(t)$, and $\varphi_2(t)$ are sufficiently smooth functions.

2 Discretization

The domain is discretized using a uniform mesh that divides the whole domain into equal subintervals to analyze the considered problem. The space domain Ω_x is discretized as $\{x_n = a + nh \mid n = 0, 1, \dots, N, h = \frac{b-a}{N}\}$ and the time domain with uniform partition is defined as $\{t_m = m\tau \mid m = 0, 1, \dots, M, \tau = \frac{T}{M}\}$, where N and M are the number of knots in the space and time directions, respectively.

2.1 Fractional derivative discretization

The fractional derivative is discretized using a quadrature formula that is given as [6, 8]

$$\begin{aligned} D_t^{\alpha_1} u(x_n, t_m) &= \frac{1}{\Gamma(1 - \alpha_1)} \int_0^{t_m} \frac{\partial u(x_n, s)}{\partial t} (t_m - s)^{-\alpha_1} ds \\ &= \frac{1}{\Gamma(1 - \alpha_1)} \sum_{k=1}^m \int_{(k-1)\tau}^{k\tau} \left[\frac{u_n^m - u_n^{m-1}}{\tau} + O(\tau) \right] (m\tau - s)^{-\alpha_1} ds \\ &= \frac{1}{\Gamma(2 - \alpha_1)} \frac{1}{\tau^{\alpha_1}} \sum_{k=1}^m (u_n^m - u_n^{m-1}) \\ &\quad [(m - k + 1)^{1-\alpha_1} - (m - k)^{1-\alpha_1}] + R_n^m(\alpha_1). \end{aligned}$$

So, we obtain the following discretized expression

$$D_t^{\alpha_1} u_n^m = \sigma_{\alpha_1} \sum_{k=1}^m d_k^{\alpha_1} (u_n^{m-k+1} - u_n^{m-k}) + R_n^m(\alpha_1), \quad (2.1)$$

where $\sigma_{\alpha_1} = \frac{1}{\Gamma(2 - \alpha_1)\tau^{\alpha_1}}$, $d_k^{\alpha_1} = k^{\alpha_1} - (k - 1)^{\alpha_1}$, and the error term $R_n^m(\alpha_1)$ is given by

$$\begin{aligned} R_n^m(\alpha_1) &= \frac{1}{\Gamma(2 - \alpha_1)} \sum_{k=1}^m [(m - k + 1)^{1-\alpha_1} - (m - k)^{1-\alpha_1}] O(\tau^{2-\alpha_1}) \\ &= \frac{1}{\Gamma(2 - \alpha_1)} m^{1-\alpha_1} O(\tau^{2-\alpha_1}) \\ &\leq CO(\tau), \end{aligned}$$

where C is a constant.

Likewise, we obtain the following expression for another fractional derivative used in the considered problem,

$$D_t^{\alpha_2} v_n^m = \sigma_{\alpha_2} \sum_{k=1}^m d_k^{\alpha_2} (v_n^{m-k+1} - v_n^{m-k}) + R_n^m(\alpha_2), \quad (2.2)$$

where $R_n^m(\alpha_2) \leq CO(\tau)$, for some constant C .

2.2 Methodology

Recently, the spline function has been widely used to solve many mathematical problems in applied sciences. The solution that is determined approximately is expressed as the linear combination of cubic B-spline basis functions. The approximations $U(x, t)$ and $V(x, t)$ to the exact solution $u(x, t)$ and $v(x, t)$ at any time t is given by

$$U_n(x, t) = \sum_{n=-1}^{N+1} \Theta_n \mathcal{B}_n(x), \quad V_n(x, t) = \sum_{n=-1}^{N+1} \Delta_n \mathcal{B}_n(x), \quad (2.3)$$

where Θ_n and Δ_n are time-dependent functions that are evaluated by utilizing the boundary conditions and the collocation form of the fractional differential equations.

The cubic B-spline basis functions at nodal points are defined as:

$$\mathcal{B}_n(x) = \begin{cases} (x - x_{n-2})^3, & x \in [x_{n-2}, x_{n-1}), \\ (x - x_{n-2})^3 - 4(x - x_{n-1})^3, & x \in [x_{n-1}, x_n), \\ (x_{n+2} - x)^3 - 4(x_{n+1} - x)^3, & x \in [x_n, x_{n+1}), \\ (x_{n+2} - x)^3, & x \in [x_{n+1}, x_{n+2}), \\ 0, & \text{otherwise,} \end{cases} \quad (2.4)$$

where $\mathcal{B}_{-1}, \mathcal{B}_0, \dots, \mathcal{B}_N, \mathcal{B}_{N+1}$ form a basis over the region $a \leq x \leq b$. The values of $\mathcal{B}_n(x)$ and its derivatives are evaluated using these basis functions and are presented in Table 1.

2.3 Problem discretization

The discretized form of the problem is given by

$$\begin{aligned} D_t^{\alpha_1} u_n^m &= (u_{xx})_n^m + \kappa (u^p u_x)_n^m - \rho_1 ((uv)_x)_n^m + f_n^m, \\ D_t^{\alpha_2} v_n^m &= (v_{xx})_n^m + \kappa (v^p v_x)_n^m - \rho_2 ((uv)_x)_n^m + g_n^m, \end{aligned}$$

that gives the following expression

$$\begin{aligned} \sigma_{\alpha_1} \sum_{k=1}^m d_k^{\alpha_1} (u_n^{m-k+1} - u_n^{m-k}) - (u_{xx})_n^m - k (u^p u_x)_n^m \\ = -\rho_1 (u_n^{m-1} (v_x)_n^{m-1} + v_n^{m-1} (u_x)_n^{m-1}) + f_n^m, \end{aligned} \quad (2.5a)$$

$$\begin{aligned} \sigma_{\alpha_2} \sum_{k=1}^m d_k^{\alpha_2} (v_n^{m-k+1} - v_n^{m-k}) - (v_{xx})_n^m - k (v^p v_x)_n^m \\ = -\rho_2 (u_n^{m-1} (v_x)_n^{m-1} + v_n^{m-1} (u_x)_n^{m-1}) + g_n^m, \end{aligned} \quad (2.5b)$$

with the conditions $u_n^0 = \phi_1(x_n)$, $v_n^0 = \phi_2(x_n)$, $u_0^m = \psi_1(t_m)$, $v_0^m = \psi_2(t_m)$, $u_N^m = \varphi_1(t_m)$, and $v_N^m = \varphi_2(t_m)$, where $n = 0, 1, \dots, N$ and $m = 1, 2, \dots, M$. The

Table 1 $\mathcal{B}_n(x)$ and its derivatives at nodal points

	x_{n-2}	x_{n-1}	x_n	x_{n+1}	x_{n+2}
$\mathcal{B}_n(x)$	0	1	4	1	0
$\mathcal{B}'_n(x)$	0	$3/h$	0	$-3/h$	0
$\mathcal{B}''_n(x)$	0	$6/h^2$	$-12/h^2$	$6/h^2$	0

approximate values of $u(x, t)$, $v(x, t)$, and their derivatives up to the second order are calculated using the approximate functions (2.3) and the cubic B-spline functions (2.4) that are given as

$$\begin{aligned}
 U_n^m &= \Theta_{n-1}^m + 4\Theta_n^m + \Theta_{n+1}^m, \quad (U')_n^m = -\frac{3}{h}\Theta_{n-1}^m + \frac{3}{h}\Theta_{n+1}^m, \\
 (U'')_n^m &= \frac{6}{h^2}\Theta_{n-1}^m - \frac{12}{h^2}\Theta_n^m + \frac{6}{h^2}\Theta_{n+1}^m,
 \end{aligned}
 \tag{2.6a}$$

$$\begin{aligned}
 V_n^m &= \Delta_{n-1}^m + 4\Delta_n^m + \Delta_{n+1}^m, \quad (V')_n^m = -\frac{3}{h}\Delta_{n-1}^m + \frac{3}{h}\Delta_{n+1}^m, \\
 (V'')_n^m &= \frac{6}{h^2}\Delta_{n-1}^m - \frac{12}{h^2}\Delta_n^m + \frac{6}{h^2}\Delta_{n+1}^m.
 \end{aligned}
 \tag{2.6b}$$

3 Demonstration of the numerical scheme

This section presents the full discretization of the problem under consideration in terms of splines. The nonlinear terms present in the equations, such as $u^p u_x$, $v^p v_x$, and $(uv)_x$ deal with the linearization techniques discussed in [25, 29, 33]. After that, for the formulation of the numerical scheme, we substitute approximations for u and v and their derivatives using Equation (2.6a) and (2.6b) in (2.5a) and (2.5b), respectively. The Equations (2.5a) and (2.5b) can be rewritten as

$$\begin{aligned}
 &\sigma_{\alpha_1} d_1^{\alpha_1} u_n^m - (u_{xx})_n^m - \kappa p (u_n^{m-1})^{p-1} (u_x)_n^{m-1} u_n^m \\
 &\quad - \kappa (u_n^{m-1})^p (u_x)_n^m = -\kappa p (u_n^{m-1})^p (u_x)_n^{m-1} \\
 &\quad + \sigma_{\alpha_1} d_m^{\alpha_1} u_n^0 + \sigma_{\alpha_1} \sum_{k=1}^{m-1} (d_k^{\alpha_1} - d_{k+1}^{\alpha_1}) u_n^{m-k} \\
 &\quad - \varrho_1 (u_n^{m-1} (v_x)_n^{m-1} + v_n^{m-1} (u_x)_n^{m-1}) + f_n^m,
 \end{aligned}
 \tag{3.1a}$$

$$\begin{aligned}
 &\sigma_{\alpha_2} d_1^{\alpha_2} v_n^m - (v_{xx})_n^m - \kappa p (v_n^{m-1})^{p-1} (v_x)_n^{m-1} v_n^m \\
 &\quad - \kappa (v_n^{m-1})^p (v_x)_n^m = -\kappa p (v_n^{m-1})^p (v_x)_n^{m-1} \\
 &\quad + \sigma_{\alpha_2} d_m^{\alpha_2} v_n^0 + \sigma_{\alpha_2} \sum_{k=1}^{m-1} (d_k^{\alpha_2} - d_{k+1}^{\alpha_2}) v_n^{m-k} \\
 &\quad - \varrho_2 (u_n^{m-1} (v_x)_n^{m-1} + v_n^{m-1} (u_x)_n^{m-1}) + g_n^m.
 \end{aligned}
 \tag{3.1b}$$

After putting the spline approximations to Equations (3.1a) and (3.1b), we obtain the following difference equations in terms of Θ_n^m and Δ_n^m , where the left-hand side of the equations involve terms at the m -th time level

$$\begin{aligned} & r_1(\Theta_{n-1}^m + 4\Theta_n^m + \Theta_{n+1}^m) + r_2(\Theta_{n-1}^m - \Theta_{n+1}^m) - r_3(\Theta_{n-1}^m - 2\Theta_n^m + \Theta_{n+1}^m) \\ &= r_4(\Theta_{n-1}^{m-1} - \Theta_{n+1}^{m-1}) \\ &+ r_5(\Delta_{n-1}^{m-1} - \Delta_{n+1}^{m-1}) + \sigma_{\alpha_1} d_m^{\alpha_1} (\Theta_{n-1}^0 + 4\Theta_n^0 + \Theta_{n+1}^0) \\ &+ \sigma_{\alpha_1} \sum_{k=1}^{m-1} (d_k^{\alpha_1} - d_{k+1}^{\alpha_1}) (\Theta_{n-1}^{m-k} + 4\Theta_n^{m-k} + \Theta_{n+1}^{m-k}), \end{aligned} \quad (3.2a)$$

$$\begin{aligned} & s_1(\Delta_{n-1}^m + 4\Delta_n^m + \Delta_{n+1}^m) + s_2(\Delta_{n-1}^m - \Delta_{n+1}^m) - s_3(\Delta_{n-1}^m - 2\Delta_n^m + \Delta_{n+1}^m) \\ &= s_4(\Delta_{n-1}^{m-1} - \Delta_{n+1}^{m-1}) \\ &+ s_5(\Theta_{n-1}^{m-1} - \Theta_{n+1}^{m-1}) + \sigma_{\alpha_2} d_m^{\alpha_2} (\Delta_{n-1}^0 + 4\Delta_n^0 + \Delta_{n+1}^0) \\ &+ \sigma_{\alpha_2} \sum_{k=1}^{m-1} (d_k^{\alpha_2} - d_{k+1}^{\alpha_2}) (\Delta_{n-1}^{m-k} + 4\Delta_n^{m-k} + \Delta_{n+1}^{m-k}), \end{aligned} \quad (3.2b)$$

where

$$\begin{aligned} r_1 &= \sigma_{\alpha_1} d_1^{\alpha_1} - \kappa p (U_n^{m-1})^{p-1} (U_x)_n^{m-1}, \quad r_2 = \frac{3\kappa (U_n^{m-1})^p}{h}, \\ r_3 &= \frac{6}{h^2}, \quad r_4 = \frac{3\kappa p (U_n^{m-1})^p}{h} + \frac{3\varrho_1 V_n^{m-1}}{h}, \\ r_5 &= \frac{3\varrho_1 U_n^{m-1}}{h}, \quad s_1 = \sigma_{\alpha_2} d_1^{\alpha_2} - \kappa p (V_n^{m-1})^{p-1} (V_x)_n^{m-1}, \\ s_2 &= \frac{3\kappa (V_n^{m-1})^p}{h}, \quad s_3 = \frac{6}{h^2}, \\ s_4 &= \frac{3\kappa p (V_n^{m-1})^p}{h} + \frac{3\varrho_2 U_n^{m-1}}{h}, \quad s_5 = \frac{3\varrho_2 V_n^{m-1}}{h}. \end{aligned}$$

3.1 Initial vector

The approximate solutions are obtained using the recurrence relation by solving the numerical scheme (3.2) at every time step. An initial vector is obtained from the initial and boundary conditions to estimate the approximations using splines.

Using the initial condition $u(x_n, 0) = \phi_1(x_n)$, $n = 0, 1, \dots, N$, and the spline approximations, we obtain $(N + 1)$ equations involving $(N + 3)$ unknowns. The two unknowns acquired by putting $n = 0$ and $n = N$ that is Θ_{-1} and Θ_{N+1} can be computed from $u_x(x_0, 0) = \phi_1'(x_0)$ and $u_x(x_N, 0) = \phi_1'(x_N)$, respectively. Thus, the $(N + 1)$ equations with $(N + 1)$ unknowns that can be solved using the Thomas algorithm are obtained.

Table 2 Errors in the L_2 and L_∞ norms and orders of convergence of $u(x, t)$ in the spatial direction for Example 5.1, for distinct p and (α_1, α_2) values

p	Norms	(α_1, α_2)	Number of nodal points				
			$N=4$ $M=16$	$N=8$ $M=64$	$N=16$ $M=256$	$N=32$ $M=1024$	
1	L_2	(0.1, 0.4)	1.2347e-02 1.6757	3.8536e-03 1.9163	1.0190e-03 1.9831	2.5838e-04	
		(0.2, 0.5)	1.2015e-02 1.6704	3.7671e-03 1.9175	9.9767e-04 1.9799	2.5315e-04	
		(0.3, 0.6)	1.1595e-02 1.6642	3.6619e-03 1.9113	9.7254e-04 1.9779	2.4709e-04	
	L_∞	(0.1, 0.4)	1.6708e-02 1.6777	5.2239e-03 1.8986	1.4035e-03 1.9755	3.5585e-04	
		(0.2, 0.5)	1.6242e-02 1.6646	5.1086e-03 1.8991	1.3738e-03 1.9729	3.4855e-04	
		(0.3, 0.6)	1.5653e-02 1.6594	4.9697e-03 1.8910	1.3388e-03 1.9786	3.4011e-04	
	2	L_2	(0.1, 0.4)	1.1508e-02 1.6090	3.7723e-03 1.9002	1.0109e-03 1.9745	2.5722e-04
			(0.2, 0.5)	1.1205e-02 1.6018	3.6902e-03 1.8981	9.9039e-04 1.9740	2.5215e-04
			(0.3, 0.6)	1.0819e-02 1.5890	3.5903e-03 1.8939	9.6620e-04 1.9734	2.4630e-04
L_∞		(0.1, 0.4)	1.5685e-02 1.6137	5.1326e-03 1.8943	1.3811e-03 1.9710	3.5216e-04	
		(0.2, 0.5)	1.5260e-02 1.6078	5.0167e-03 1.8947	1.3530e-03 1.9683	3.4507e-04	
		(0.3, 0.6)	1.4719e-02 1.5909	4.8757e-03 1.8863	1.3199e-03 1.9697	3.3688e-04	

Likewise, the initial vector for v can be evaluated using the initial condition $v(x_n, 0) = \phi_2(x_n)$, $n = 0, 1, \dots, N$.

4 Stability analysis

In this section, the stability of the proposed scheme is demonstrated through the Von-Neumann stability analysis method. The non-linear terms $u^p u_x$, $v^p v_x$ and $(uv)_x$ are linearized by assuming U_n^{m-1} and V_n^{m-1} as local constants \hat{U} and \hat{V} . To begin the analysis of the stability of the scheme, let the error term be defined as $e_n^m = \Theta_n^m - \tilde{\Theta}_n^m$, $n = 0, 1, \dots, N$, $m = 0, 1, \dots, M$, where Θ_n^m and $\tilde{\Theta}_n^m$ are the growth

Table 3 Errors in the L_2 and L_∞ norms and orders of convergence of $v(x, t)$ in the spatial direction for Example 5.1, for distinct p and (α_1, α_2) values

p	Norms	(α_1, α_2)	Number of nodal points			
			$N=4$ $M=16$	$N=8$ $M=64$	$N=16$ $M=256$	$N=32$ $M=1024$
1	L_2	(0.1, 0.4)	1.1122e - 02	3.5568e - 03	9.4873e - 04	2.4148e - 04
			1.6406	1.9074	1.9774	
		(0.2, 0.5)	1.0435e - 02	3.3954e - 03	9.1251e - 04	2.3322e - 04
			1.6130	1.8968	1.9703	
		(0.3, 0.6)	9.5212e - 03	3.1789e - 03	8.6463e - 04	2.2261e - 04
			1.5819	1.8783	1.9557	
	L_∞	(0.1, 0.4)	1.5030e - 02	4.8157e - 03	1.3050e - 03	3.3213e - 04
			1.6379	1.8795	1.9803	
		(0.2, 0.5)	1.4087e - 02	4.5989e - 03	1.2546e - 03	3.2061e - 04
			1.6160	1.8797	1.9613	
		(0.3, 0.6)	1.2833e - 02	4.3080e - 03	1.1882e - 03	3.0587e - 04
			1.5704	1.8567	1.9594	
2	L_2	(0.1, 0.4)	1.0371e - 02	3.4854e - 03	9.4192e - 04	2.4055e - 04
			1.5753	1.8894	1.9667	
		(0.2, 0.5)	9.7258e - 03	3.3298e - 03	9.0669e - 04	2.3250e - 04
			1.5469	1.8763	1.9608	
		(0.3, 0.6)	8.8556e - 03	3.1195e - 03	8.5984e - 04	2.2212e - 04
			1.5058	1.8591	1.9538	
	L_∞	(0.1, 0.4)	1.4121e - 02	4.7359e - 03	1.2853e - 03	3.2889e - 04
			1.5727	1.8775	1.9712	
		(0.2, 0.5)	1.3232e - 02	4.5201e - 03	1.2369e - 03	3.1767e - 04
			1.5461	1.8660	1.9632	
		(0.3, 0.6)	1.2037e - 02	4.2298e - 03	1.1727e - 03	3.0326e - 04
			1.5043	1.8541	1.9491	

factor and its approximation in Fourier mode, respectively. Using (3.2a), the error equation is written as

$$\zeta_1 \epsilon_{n-1}^m + \zeta_2 \epsilon_n^m + \zeta_3 \epsilon_{n+1}^m = \zeta_4 (\epsilon_{n-1}^0 + 4\epsilon_n^0 + \epsilon_{n+1}^0) + \zeta_k (\epsilon_{n-1}^{m-k} + 4\epsilon_n^{m-k} + \epsilon_{n+1}^{m-k}), \tag{4.1}$$

$0 \leq n \leq N, 0 < m \leq M$, where $\zeta_1 = r_1 + r_2 - r_3, \zeta_2 = 4r_1 + 2r_3, \zeta_3 = r_1 - r_2 - r_3, \zeta_4 = \sigma_{\alpha_1} d_m^{\alpha_1}$, and $\zeta_k = \sigma_{\alpha_1} \sum_{k=1}^{m-1} (d_k^{\alpha_1} - d_{k+1}^{\alpha_1})$. Now, the grid function is defined as

$$\epsilon^m(x) = \begin{cases} \epsilon_n^m, & x_n - \frac{h}{2} < x < x_n + \frac{h}{2}, \quad n = 1, 2, \dots, N - 1, \\ 0, & a \leq x \leq a + \frac{h}{2} \text{ or } b - \frac{h}{2} \leq x \leq b. \end{cases}$$

Taking $\Omega_x = (a, b) = (0, L)$, the Fourier series expansion is given as

Table 4 Errors in the L_2 and L_∞ norms and orders of convergence in the temporal direction for Example 5.1, for $p = 1$ with different ordered pairs (α_1, α_2)

(α_1, α_2)	Norms	Number of nodal points				
		$N=32$ $M=20$	$N=64$ $M=40$	$N=128$ $M=80$	$N=256$ $M=160$	$N=512$ $M=320$
(0.5, 0.8)	$L_2(u)$	$9.5114e - 03$	$5.4473e - 03$	$2.9230e - 03$	$1.5177e - 03$	$7.7478e - 04$
		0.8032	0.9003	0.9419	0.9718	
	$L_\infty(u)$	$1.3120e - 02$	$7.5063e - 03$	$4.0255e - 03$	$2.0894e - 03$	$1.0664e - 03$
		0.8027	0.8980	0.9473	0.9659	
(0.5, 0.5)	$L_2(v)$	$6.4723e - 03$	$3.9184e - 03$	$2.1768e - 03$	$1.1598e - 03$	$6.0458e - 04$
		0.7229	0.8465	0.9102	0.9391	
	$L_\infty(v)$	$8.9288e - 03$	$5.3926e - 03$	$2.9931e - 03$	$1.5938e - 03$	$8.3054e - 04$
		0.7284	0.8501	0.9111	0.9361	
(0.8, 0.5)	$L_2(u)$	$9.5898e - 03$	$5.4918e - 03$	$2.9459e - 03$	$1.5290e - 03$	$7.8017e - 04$
		0.8047	0.8961	0.9472	0.9720	
	$L_\infty(u)$	$1.3210e - 02$	$7.5616e - 03$	$4.0542e - 03$	$2.1036e - 03$	$1.0732e - 03$
		0.8041	0.9005	0.9475	0.9728	
(0.8, 0.5)	$L_2(v)$	$9.5898e - 03$	$5.4918e - 03$	$2.9459e - 03$	$1.5290e - 03$	$7.8017e - 04$
		0.8047	0.8961	0.9472	0.9720	
	$L_\infty(v)$	$1.3210e - 02$	$7.5616e - 03$	$4.0542e - 03$	$2.1036e - 03$	$1.0732e - 03$
		0.8041	0.9005	0.9475	0.9728	
(0.8, 0.5)	$L_2(u)$	$6.4723e - 03$	$3.9184e - 03$	$2.1768e - 03$	$1.1598e - 03$	$6.0458e - 04$
		0.7229	0.8465	0.9102	0.9391	
	$L_\infty(u)$	$8.9288e - 03$	$5.3926e - 03$	$2.9931e - 03$	$1.5938e - 03$	$8.3054e - 04$
		0.7284	0.8501	0.9111	0.9361	
(0.8, 0.5)	$L_2(v)$	$9.5114e - 03$	$5.4473e - 03$	$2.9230e - 03$	$1.5177e - 03$	$7.7478e - 04$
		0.8032	0.9003	0.9419	0.9718	
	$L_\infty(v)$	$1.3120e - 02$	$7.5063e - 03$	$4.0255e - 03$	$2.0894e - 03$	$1.0664e - 03$
		0.8027	0.8980	0.9473	0.9659	

$$e^m(x) = \sum_{j=-\infty}^{\infty} \delta_m(j) e^{i \frac{2\pi j x}{L}}, \quad m = 0, 1, \dots, M,$$

where

$$\delta_m(j) = \frac{1}{L} \int_0^L e^m(\theta) e^{-i \frac{2\pi j \theta}{L}} d\theta,$$

are the Fourier coefficients.

Now, using the norm and Parseval’s equality, we obtain

Table 5 Errors in the L_2 and L_∞ norms and orders of convergence in the temporal direction for Example 5.1, for $p = 2$ with different ordered pairs (α_1, α_2)

(α_1, α_2)	Norms	Number of nodal points				
		$N=32$ $M=20$	$N=64$ $M=40$	$N=128$ $M=80$	$N=256$ $M=160$	$N=512$ $M=320$
(0.5, 0.8)	$L_2(u)$	$9.0761e - 03$	$5.3166e - 03$	$2.8880e - 03$	$1.5091e - 03$	$7.7280e - 04$
		0.7713	0.8804	0.9365	0.9660	
	$L_\infty(u)$	$1.2424e - 02$	$7.2730e - 03$	$3.9497e - 03$	$2.0635e - 03$	$1.0566e - 03$
		0.7703	0.8801	0.9392	0.9586	
	$L_2(v)$	$6.1116e - 03$	$3.8113e - 03$	$2.1484e - 03$	$1.1529e - 03$	$6.0312e - 04$
		0.6814	0.8255	0.9027	0.9314	
	$L_\infty(v)$	$8.3588e - 03$	$5.2066e - 03$	$2.9329e - 03$	$1.5734e - 03$	$8.2296e - 04$
		0.6822	0.8304	0.9001	0.9318	
(0.5, 0.5)	$L_2(u)$	$9.1391e - 03$	$5.3518e - 03$	$2.9060e - 03$	$1.5179e - 03$	$7.7701e - 04$
		0.7727	0.8785	0.9369	0.9681	
	$L_\infty(u)$	$1.2501e - 02$	$7.3176e - 03$	$3.9728e - 03$	$2.0748e - 03$	$1.0621e - 03$
		0.7720	0.8827	0.9395	0.9656	
	$L_2(v)$	$9.1391e - 03$	$5.3518e - 03$	$2.9060e - 03$	$1.5179e - 03$	$7.7701e - 04$
		0.7727	0.8785	0.9369	0.9681	
	$L_\infty(v)$	$1.2501e - 02$	$7.3176e - 03$	$3.9728e - 03$	$2.0748e - 03$	$1.0621e - 03$
		0.7720	0.8827	0.9395	0.9656	
(0.8, 0.5)	$L_2(u)$	$6.1116e - 03$	$3.8113e - 03$	$2.1484e - 03$	$1.1529e - 03$	$6.0312e - 04$
		0.6814	0.8255	0.9027	0.9314	
	$L_\infty(u)$	$8.3588e - 03$	$5.2066e - 03$	$2.9329e - 03$	$1.5734e - 03$	$8.2296e - 04$
		0.6822	0.8304	0.9001	0.9318	
	$L_2(v)$	$9.0761e - 03$	$5.3166e - 03$	$2.8880e - 03$	$1.5091e - 03$	$7.7280e - 04$
		0.7713	0.8804	0.9365	0.9660	
	$L_\infty(v)$	$1.2424e - 02$	$7.2730e - 03$	$3.9497e - 03$	$2.0635e - 03$	$1.0566e - 03$
		0.7703	0.8801	0.9392	0.9586	

$$\|\epsilon^m\|_2^2 = \left(\sum_{n=1}^{N-1} h|\epsilon_n^m|^2 \right) = \left(\int_0^L |\epsilon^m(x)|^2 dx \right) = L \sum_{j=-\infty}^{\infty} |\delta_m(j)|^2. \tag{4.2}$$

Let $\epsilon_n^m = \delta_m e^{inj\gamma}$, where $L = 1$, and $\gamma = 2\pi j/L$ is the wave number.

Lemma 4.1 For $\alpha_1, \alpha_2 \in (0, 1)$, the inequality $|\delta_m| \leq |\delta_0|$ holds true for $m = 1, 2, \dots, M$.

Proof From Equation (4.1), for $m = 1$ we get

$$(\zeta_1 e^{i(n-1)h\gamma} + \zeta_2 e^{inh\gamma} + \zeta_3 e^{i(n+1)h\gamma})\delta_1 = \zeta_4 (e^{i(n-1)h\gamma} + 4e^{inh\gamma} + e^{i(n+1)h\gamma})\delta_0.$$

On simplification, which gives

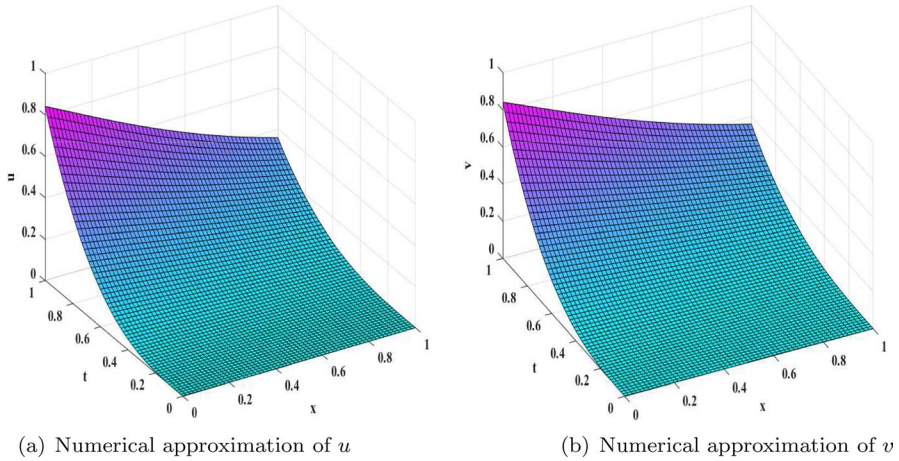


Fig. 1 Numerical solutions at $(\alpha_1, \alpha_2) = (0.5, 0.5)$, $p = 2$, and $N = M = 60$ for Example 5.1

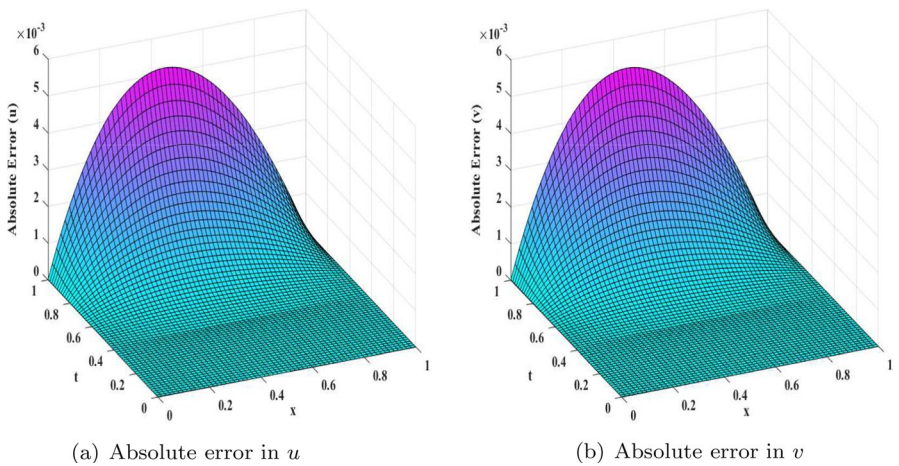


Fig. 2 Absolute errors at $(\alpha_1, \alpha_2) = (0.5, 0.5)$, $p = 2$, and $N = M = 60$ for Example 5.1

$$|((\zeta_1 + \zeta_3) \cos(h\gamma) + i(-\zeta_1 + \zeta_3) \sin(h\gamma) + \zeta_2)\delta_1| = |\zeta_4(2 \cos(h\gamma) + 4)\delta_0|,$$

that gives

$$|\delta_1| = \frac{|\zeta_4(2 \cos(h\gamma) + 4)|}{|(\zeta_1 + \zeta_3) \cos(h\gamma) + i(-\zeta_1 + \zeta_3) \sin(h\gamma) + \zeta_2|} |\delta_0|.$$

Thus, we obtain $|\delta_1| \leq |\delta_0|$ as $\tau \rightarrow 0$.

Now, assume that the inequality $|\delta_q| \leq |\delta_0|$ holds for $q = 2, 3, \dots, m - 1$.

Then for $q = m$, we have

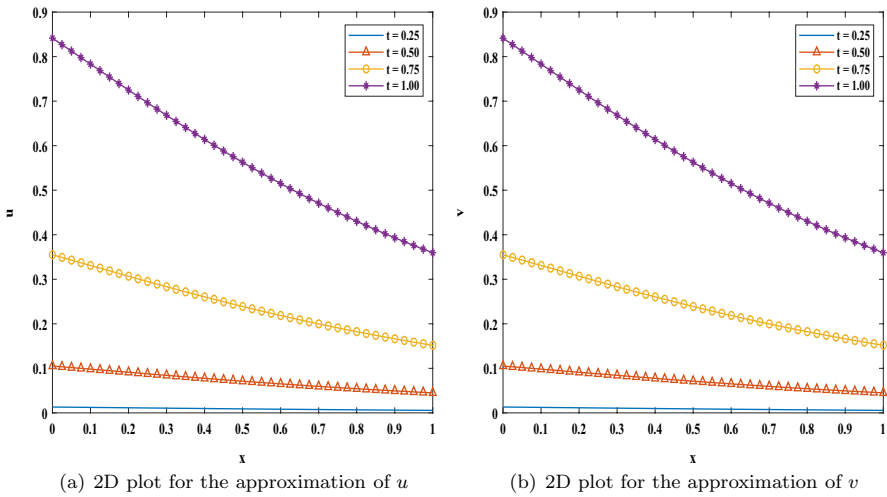


Fig. 3 Numerical solutions at distinct time levels when $(\alpha_1, \alpha_2) = (0.5, 0.5)$, $p = 2$, and $N = M = 40$ for Example 5.1

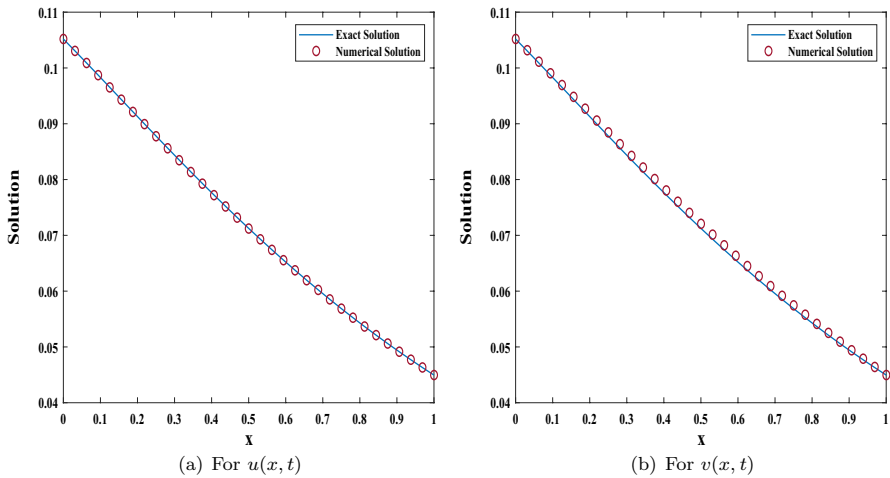


Fig. 4 Exact and numerical solutions when $(\alpha_1, \alpha_2) = (0.5, 0.8)$, $p = 2$, and $N = M = 32$ at $t = 0.5$ for Example 5.1

$$\begin{aligned}
 (\zeta_1 e^{i(n-1)h\gamma} + \zeta_2 e^{inh\gamma} + \zeta_3 e^{i(n+1)h\gamma})\delta_m &= \zeta_4 (e^{i(n-1)h\gamma} + 4e^{inh\gamma} + e^{i(n+1)h\gamma})\delta_0 \\
 &+ \zeta_k (e^{i(n-1)h\gamma} + 4e^{inh\gamma} + e^{i(n+1)h\gamma})\delta_{m-k}.
 \end{aligned}$$

Taking absolute values, which gives

Table 6 Errors in the L_2 and L_∞ norms and orders of convergence of $u(x, t)$ in the spatial direction for Example 5.2, for distinct p and (α_1, α_2) values

p	Norms	(α_1, α_2)	Number of nodal points				
			$N=4$ $M=16$	$N=8$ $M=64$	$N=16$ $M=256$	$N=32$ $M=1024$	
3	L_2	(0.2, 0.5)	3.2145E - 03 1.5196	1.1212E - 03 1.8860	3.0335E - 04 1.9715	7.7352E - 05	
		(0.3, 0.6)	3.1923E - 03 1.5230	1.1108E - 03 1.8862	3.0049E - 04 1.9711	7.6645E - 05	
		(0.4, 0.7)	3.1719E - 03 1.5309	1.0977E - 03 1.8872	2.9675E - 04 1.9706	7.5716E - 05	
	L_∞	(0.2, 0.5)	4.8288e - 03 1.5088	1.6969e - 03 1.8862	4.5905e - 04 1.9721	1.1700e - 04	
		(0.3, 0.6)	4.8640e - 03 1.5297	1.6846e - 03 1.8912	4.5414e - 04 1.9735	1.1564e - 04	
		(0.4, 0.7)	4.9379e - 03 1.5601	1.6746e - 03 1.9000	4.4871e - 04 1.9765	1.1402e - 04	
	4	L_2	(0.2, 0.5)	3.2297e - 03 1.5247	1.1225e - 03 1.8876	3.0337e - 04 1.9719	7.7335e - 05
			(0.3, 0.6)	3.2073e - 03 1.5282	1.1120e - 03 1.8877	3.0051e - 04 1.9715	7.6629e - 05
			(0.4, 0.7)	3.1866e - 03 1.5360	1.0989e - 03 1.8886	2.9677e - 04 1.9710	7.5701e - 05
L_∞		(0.2, 0.5)	4.8510e - 03 1.5135	1.6991e - 03 1.8878	4.5912e - 04 1.9721	1.1702e - 04	
		(0.3, 0.6)	4.8856e - 03 1.5343	1.6867e - 03 1.8928	4.5420e - 04 1.9739	1.1562e - 04	
		(0.4, 0.7)	4.9589e - 03 1.5645	1.6766e - 03 1.9016	4.4875e - 04 1.9769	1.1400e - 04	

$$|\delta_m| \leq \frac{|(2 \cos(h\gamma) + 4)|(\zeta_4|\delta_0| + \zeta_k|\delta_{m-k})|}{|(\zeta_1 + \zeta_3) \cos(h\gamma) + i(-\zeta_1 + \zeta_3) \sin(h\gamma) + \zeta_2|}$$

Note that $d_m^{\alpha_1} + \sum_{k=1}^{m-1} (d_k^{\alpha_1} - d_{k+1}^{\alpha_1}) = d_1^{\alpha_1}$, we get

$$|\delta_m| \leq \frac{2\sigma_{\alpha_1} d_1^{\alpha_1} (2 \cos(h\gamma) + 4)}{|(\zeta_1 + \zeta_3) \cos(h\gamma) + i(-\zeta_1 + \zeta_3) \sin(h\gamma) + \zeta_2|} |\delta_0|$$

As the time step τ approaches zero, we get $|\delta_m| \leq |\delta_0|$.

Hence, the lemma is proved by utilizing the concept of mathematical induction. □

Table 7 Errors in the L_2 and L_∞ norms and orders of convergence of $v(x, t)$ in the spatial direction for Example 5.2, for distinct p and (α_1, α_2) values

p	Norms	(α_1, α_2)	Number of nodal points			
			$N=4$ $M=16$	$N=8$ $M=64$	$N=16$ $M=256$	$N=32$ $M=1024$
3	L_2	(0.2, 0.5)	$3.2305E - 03$	$1.1021E - 03$	$2.9571E - 04$	$7.5124E - 05$
			1.5515	1.8980	1.9768	
		(0.3, 0.6)	$3.2938E - 03$	$1.1002E - 03$	$2.9345E - 04$	$7.4340E - 05$
	L_∞	(0.2, 0.5)	1.5820	1.9066	1.9809	
			$3.4667E - 03$	$1.1138E - 03$	$2.9338E - 04$	$7.3849E - 05$
		(0.3, 0.6)	1.6381	1.9246	1.9901	
	L_2	(0.2, 0.5)	$5.1749e - 03$	$1.7029e - 03$	$4.4969e - 04$	$1.1332e - 04$
			1.6035	1.9210	1.9885	
		(0.3, 0.6)	$5.4551e - 03$	$1.7363e - 03$	$4.5188e - 04$	$1.1291e - 04$
L_∞	(0.2, 0.5)	1.6516	1.9420	2.0008		
		$5.9031e - 03$	$1.8121e - 03$	$4.6353e - 04$	$1.1468e - 04$	
	(0.3, 0.6)	1.7038	1.9669	2.0150		
4	L_2	(0.2, 0.5)	$3.2447e - 03$	$1.1032e - 03$	$2.9572e - 04$	$7.5106e - 05$
			1.5564	1.8994	1.9772	
		(0.3, 0.6)	$3.3071e - 03$	$1.1013e - 03$	$2.9345e - 04$	$7.4322e - 05$
	L_∞	(0.2, 0.5)	1.5864	1.9080	1.9813	
			$3.4786e - 03$	$1.1148e - 03$	$2.9338e - 04$	$7.3831e - 05$
		(0.3, 0.6)	1.6417	1.9259	1.9905	
	L_2	(0.2, 0.5)	$5.1950e - 03$	$1.7046e - 03$	$4.4968e - 04$	$1.1329e - 04$
			1.6077	1.9225	1.9889	
		(0.3, 0.6)	$5.4741e - 03$	$1.7377e - 03$	$4.5183e - 04$	$1.1289e - 04$
L_∞	(0.2, 0.5)	1.6554	1.9433	2.0009		
		$5.9205e - 03$	$1.8131e - 03$	$4.6341e - 04$	$1.1465e - 04$	
	(0.3, 0.6)	1.7073	1.9681	2.0151		

Theorem 4.1 *The proposed implicit spline-based numerical scheme for time-fractional coupled Burgers’ equation defined by Equation (3.2a) is unconditionally stable.*

Proof From the Equation (4.2) and Lemma 4.1, we get the following inequality

$$\|e^m\|^2 \leq \|e^0\|^2, \text{ for } m = 1, 2, \dots, M.$$

Hence, the presented numerical scheme defined in (3.2a) is unconditionally stable. □

Remark 4.1 For the Equation (3.2b), a similar process is followed to prove the stability.

Table 8 Errors in the L_2 and L_∞ norms and orders of convergence in the temporal direction for Example 5.2, for $p = 3$ with different ordered pairs (α_1, α_2)

(α_1, α_2)	Norms	Number of nodal points				
		$N=32$ $M=20$	$N=64$ $M=40$	$N=128$ $M=80$	$N=256$ $M=160$	$N=512$ $M=320$
(0.4, 0.7)	$L_2(u)$	$3.2720e - 03$	$1.7850e - 03$	$9.3219e - 04$	$4.7646e - 04$	$2.4095e - 04$
		0.8742	0.9372	0.9683	0.9836	
	$L_\infty(u)$	$5.0065e - 03$	$2.7211e - 03$	$1.4174e - 03$	$7.2282e - 04$	$3.6484e - 04$
		0.8796	0.9409	0.9715	0.9864	
	$L_2(v)$	$3.4262e - 03$	$1.8239e - 03$	$9.3740e - 04$	$4.7358e - 04$	$2.3741e - 04$
		0.9096	0.9603	0.9851	0.9962	
	$L_\infty(v)$	$5.7440e - 03$	$3.0011e - 03$	$1.5203e - 03$	$7.5799e - 04$	$3.7560e - 04$
		0.9366	0.9811	1.0041	1.0130	
(0.5, 0.5)	$L_2(u)$	$3.2955e - 03$	$1.7903e - 03$	$9.3197e - 04$	$4.7511e - 04$	$2.3977e - 04$
		0.8803	0.9418	0.9720	0.9866	
	$L_\infty(u)$	$5.1578e - 03$	$2.7750e - 03$	$1.4333e - 03$	$7.2627e - 04$	$3.6477e - 04$
		0.8943	0.9531	0.9808	0.9935	
	$L_2(v)$	$3.2955e - 03$	$1.7903e - 03$	$9.3197e - 04$	$4.7511e - 04$	$2.3977e - 04$
		0.8803	0.9418	0.9720	0.9866	
	$L_\infty(v)$	$5.1578e - 03$	$2.7750e - 03$	$1.4333e - 03$	$7.2627e - 04$	$3.6477e - 04$
		0.8943	0.9531	0.9808	0.9935	
(0.7, 0.4)	$L_2(u)$	$3.4262e - 03$	$1.8239e - 03$	$9.3740e - 04$	$4.7358e - 04$	$2.3741e - 04$
		0.9096	0.9603	0.9851	0.9962	
	$L_\infty(u)$	$5.7440e - 03$	$3.0011e - 03$	$1.5203e - 03$	$7.5799e - 04$	$3.7560e - 04$
		0.9366	0.9811	1.0041	1.0130	
	$L_2(v)$	$3.2720e - 03$	$1.7850e - 03$	$9.3219e - 04$	$4.7646e - 04$	$2.4095e - 04$
		0.8742	0.9372	0.9683	0.9836	
	$L_\infty(v)$	$5.0065e - 03$	$2.7211e - 03$	$1.4174e - 03$	$7.2282e - 04$	$3.6484e - 04$
		0.8796	0.9409	0.9715	0.9864	

5 Numerical results

This part provides test examples to validate the theoretical conclusions and evaluate the scheme's accuracy. The numerical results in tables and graphs demonstrate that the proposed method is proficient and reliable for obtaining the numerical solutions of various time-fractional coupled nonlinear PDEs. Further, the tables show the order of convergence in both directions. The following test examples have the exact solutions used to estimate the errors in the L_2 and L_∞ norms using the formulae

Table 9 Errors in the L_2 and L_∞ norms and orders of convergence in the temporal direction for Example 5.2, for $p = 4$ with different ordered pairs (α_1, α_2)

(α_1, α_2)	Norms	Number of nodal points				
		$N=32$ $M=20$	$N=64$ $M=40$	$N=128$ $M=80$	$N=256$ $M=160$	$N=512$ $M=320$
(0.4, 0.7)	$L_2(u)$	$3.2835e - 03$	$1.7882e - 03$	$9.3294e - 04$	$4.7659e - 04$	$2.4095e - 04$
		0.8767	0.9387	0.9690	0.9840	
	$L_\infty(u)$	$5.0236e - 03$	$2.7264e - 03$	$1.4187e - 03$	$7.2310e - 04$	$3.6487e - 04$
		0.8817	0.9424	0.9723	0.9868	
	$L_2(v)$	$3.4359e - 03$	$1.8266e - 03$	$9.3799e - 04$	$4.7366e - 04$	$2.3739e - 04$
		0.9115	0.9615	0.9857	0.9966	
	$L_\infty(v)$	$5.7586e - 03$	$3.0048e - 03$	$1.5210e - 03$	$7.5800e - 04$	$3.7552e - 04$
		0.9384	0.9822	1.0048	1.0133	
(0.5, 0.5)	$L_2(u)$	$3.3066e - 03$	$1.7934e - 03$	$9.3268e - 04$	$4.7523e - 04$	$2.3976e - 04$
		0.8827	0.9432	0.9728	0.9870	
	$L_\infty(u)$	$5.1740e - 03$	$2.7798e - 03$	$1.4344e - 03$	$7.2647e - 04$	$3.6477e - 04$
		0.8963	0.9545	0.9815	0.9939	
	$L_2(v)$	$3.3066e - 03$	$1.7934e - 03$	$9.3268e - 04$	$4.7523e - 04$	$2.3976e - 04$
		0.8827	0.9432	0.9728	0.9870	
	$L_\infty(v)$	$5.1740e - 03$	$2.7798e - 03$	$1.4344e - 03$	$7.2647e - 04$	$3.6477e - 04$
		0.8963	0.9545	0.9815	0.9939	
(0.7, 0.4)	$L_2(u)$	$3.4359e - 03$	$1.8266e - 03$	$9.3799e - 04$	$4.7366e - 04$	$2.3739e - 04$
		0.9115	0.9615	0.9857	0.9966	
	$L_\infty(u)$	$5.7586e - 03$	$3.0048e - 03$	$1.5210e - 03$	$7.5800e - 04$	$3.7552e - 04$
		0.9384	0.9822	1.0048	1.0133	
	$L_2(v)$	$3.2835e - 03$	$1.7882e - 03$	$9.3294e - 04$	$4.7659e - 04$	$2.4095e - 04$
		0.8767	0.9387	0.9690	0.9840	
	$L_\infty(v)$	$5.0236e - 03$	$2.7264e - 03$	$1.4187e - 03$	$7.2310e - 04$	$3.6487e - 04$
		0.8817	0.9424	0.9723	0.9868	

$$E_2^{N,M} = \max_{1 \leq m \leq M} \sqrt{h \sum_{n=1}^N |Z(x_n, t_m) - z(x_n, t_m)|^2},$$

$$E_\infty^{N,M} = \max_{1 \leq m \leq M} \left(\max_{1 \leq n \leq N-1} |Z(x_n, t_m) - z(x_n, t_m)| \right),$$

where $z(x, t) = u(x_n, t_m)$, $v(x_n, t_m)$ are the exact solutions and $Z(x, t) = U(x_n, t_m)$, $V(x_n, t_m)$ are the approximate solutions to the problem (1.1). In addition, the order of convergence is specified as

$$O = \frac{\ln(E_q^{N,M} / E_q^{2N,2M})}{\ln 2}, \quad q = 2, \infty.$$

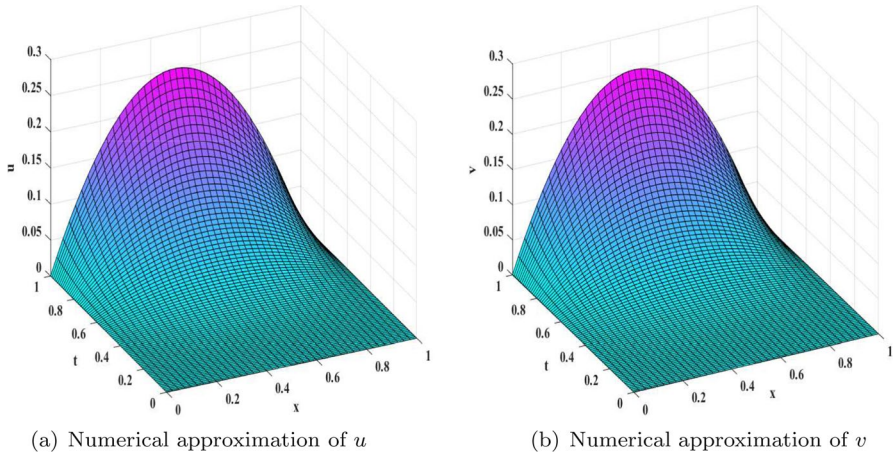


Fig. 5 Numerical solutions at $(\alpha_1, \alpha_2) = (0.3, 0.7)$, $p = 3$, and $N = M = 80$ for Example 5.2

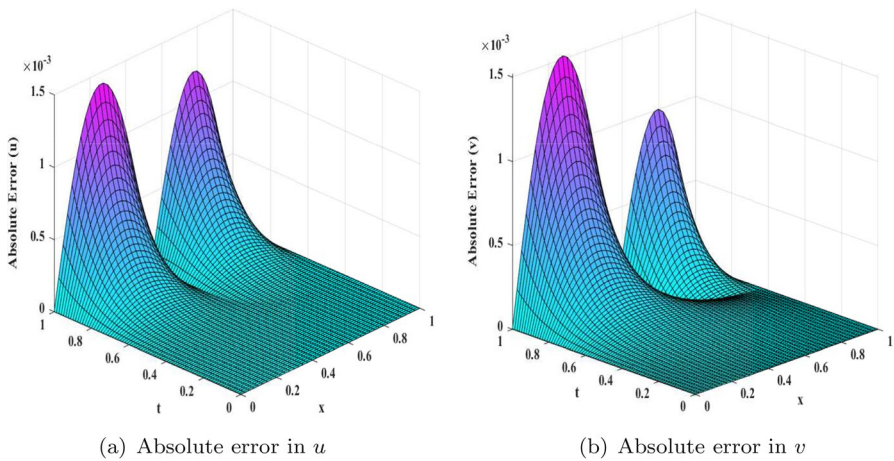


Fig. 6 Absolute errors at $(\alpha_1, \alpha_2) = (0.3, 0.7)$, $p = 3$, and $N = M = 80$ for Example 5.2

Example 5.1 Consider the problem (1.1) on $\Omega_x \times \Omega_t = (0, 1) \times (0, 1)$ with $\kappa = 2$, $\rho_1 = \rho_2 = 1$. The source terms are defined as $f(x, t) = \frac{6t^{3-\alpha_1} \sin(e^{-x})}{\Gamma(4-\alpha_1)} + t^3 e^{-2x} \sin(e^{-x}) - t^3 e^{-x} \cos(e^{-x}) + \kappa(t^3 \sin(e^{-x}))^p t^3 e^{-x} \cos(e^{-x}) - \rho_1 t^6 e^{-x} \sin(2e^{-x})$ and $g(x, t) = \frac{6t^{3-\alpha_2} \sin(e^{-x})}{\Gamma(4-\alpha_2)} + t^3 e^{-2x} \sin(e^{-x}) - t^3 e^{-x} \cos(e^{-x}) + \kappa(t^3 \sin(e^{-x}))^p t^3 e^{-x} \cos(e^{-x}) - \rho_2 t^6 e^{-x} \sin(2e^{-x})$. The initial and boundary conditions are obtained using the exact solution.

The exact solution to the above problem is $u(x, t) = v(x, t) = t^3 \sin(e^{-x})$.

The errors in the L_2 and L_∞ norms are presented in Tables 2 and 3 for three different values of α_1 and α_2 with $p = 1, 2$. From these tables, one can observe that the scheme gives second order of accuracy in the space direction. In addition,

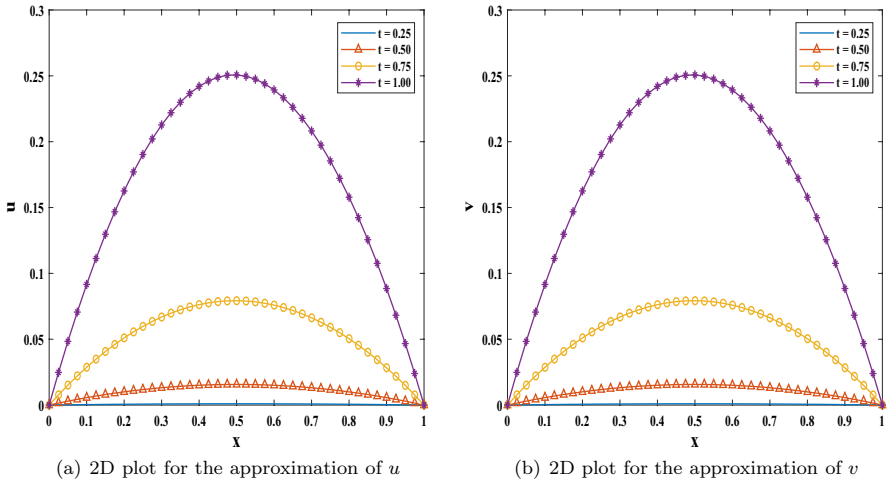


Fig. 7 Numerical solutions at distinct time levels when $(\alpha_1, \alpha_2) = (0.5, 0.5)$, $p = 3$, and $N = M = 40$ for Example 5.2

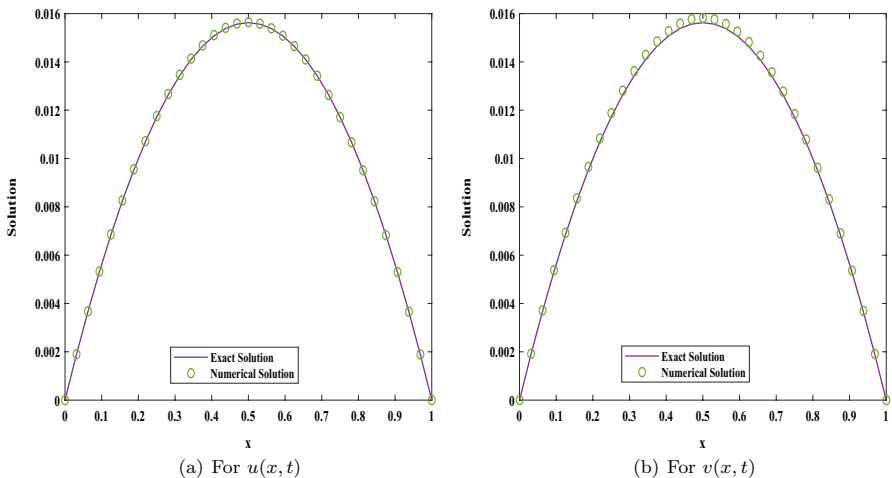


Fig. 8 Exact and numerical solutions when $(\alpha_1, \alpha_2) = (0.3, 0.7)$, $p = 4$, and $N = M = 32$ at $t = 0.5$ for Example 5.2

Tables 4 and 5 present the numerical errors and their corresponding orders in the time direction. Various numerical plots are also presented, such as Figs. 1 and 2 show the surface plots that represent the numerical solution and absolute error behavior, respectively at $(\alpha_1, \alpha_2) = (0.5, 0.5)$ and $p = 2$ with $N = M = 60$. Figure 3 shows the variations of numerical solutions at distinct time levels, and Fig. 4 presents the exact and numerical plots at $t = 0.5$.

Example 5.2 Consider the problem (1.1) on $\Omega_x \times \Omega_t = (0, 1) \times (0, 1)$ with $\kappa = 2$, $\varrho_1 = \varrho_2 = 3$. The source terms are defined as $f(x, t) = \frac{24t^{4-\alpha_1}x(1-x)}{\Gamma(5-\alpha_1)} + 2t^4 - \kappa(t^4x(1-x))^p t^4(1-2x) + \varrho_1(4x^3 - 6x^2 + 2x)$ and $g(x, t) = \frac{24t^{4-\alpha_2}x(1-x)}{\Gamma(5-\alpha_2)} + 2t^4 - \kappa(t^4x(1-x))^p t^4(1-2x) + \varrho_2(4x^3 - 6x^2 + 2x)$. The initial and boundary conditions are obtained using the exact solution.

The exact solution to the above problem is $u(x, t) = v(x, t) = t^4x(1-x)$.

The numerical errors and order of accuracy in both directions for Example 5.2 are shown in Tables 6, 7, 8 and 9 for distinct values of α_1 and α_2 . Moreover, the numerical solution surface plots are shown in Figs. 5, and 6 presents the surface plots of absolute errors that are obtained by numerical computations for Example 5.2. The graphs of numerical solutions at distinct time levels are shown in Fig. 7. The exact and numerical solutions at $t = 0.5$ for $p = 4$ are drawn together in Fig. 8.

6 Conclusion

In this work, we have investigated the time-fractional coupled generalized Burgers' equation through an implicit numerical scheme associated with the cubic B-spline technique. We used the linearization technique to change the non-linear coupled equation into a set of linear equations. The time-fractional derivative is discretized using the Caputo derivative. Moreover, through meticulous analysis, we have shown that our proposed numerical scheme is unconditionally stable. The numerical examples are presented, and the computed results are delivered through tables and graphs. The tables clearly show the correct convergence orders for different values of α_1 and α_2 . The numerical results authenticate our theoretical results and show that the numerical scheme for the fractional non-linear coupled equation is proficient and accurate and can be applied to various types of fractional coupled equations.

Author Contributions Prof. J-Vigo Aguiar did the conceptualization and methodology of the manuscript, Reetika Chawla wrote the main manuscript text, Prof. Devendra Kumar supervised and validated the file. Tapas Mazumdar has done implementation and evaluated the numerical results.

Funding This research did not receive any specific grant from funding agencies in the public, commercial, or not-for-profit sectors.

Availability of data and materials Data sharing is not applicable to this article as no data sets were generated or analyzed during the current study.

Declarations

Ethical approval Not applicable

Competing interests The authors state that they have no known competing financial interests or personal ties that could have influenced the research presented in this study.

References

1. R. Hilfer, Foundations of fractional dynamics. *Fractals* **3**, 549–556 (1995)
2. K. Oldham, J. Spanier, *The Fractional Calculus Theory and Applications of Differentiation and Integration to Arbitrary Order* (Elsevier, Amsterdam, 1974)
3. I. Podlubny, *Fractional Differential Equations* (Academic Press, San Diego, 1999)
4. S.G. Samko, A.A. Kilbas, O.I. Marichev, *Fractional Integrals and Derivatives* (Gordon and Breach Sciences Publishers, Switzerland, 1993)
5. D.B. Dhaigude, G.A. Birajdar, Numerical solution of fractional partial differential equations by discrete adomian decomposition method. *Adv. Appl. Math. Mech.* **6**, 107–119 (2014)
6. M. Uddin, S. Haq, RBFs approximation method for time fractional partial differential equations. *Commun. Nonlinear Sci. Numer. Simul.* **16**, 4208–4214 (2011)
7. R. Chawla, K. Deswal, D. Kumar, D. Baleanu, A novel finite difference based numerical approach for Modified Atangana-Baleanu Caputo derivative. *AIMS Math.* **7**, 17252–17268 (2022)
8. D.A. Murio, Implicit finite difference approximation for time fractional diffusion equations. *Comput. Math. Appl.* **56**, 1138–1145 (2008)
9. J.H. He, A short remark on fractional variational iteration method. *Phys. Lett. A* **375**, 3362–3364 (2011)
10. J.M. Burgers, A mathematical model illustrating the theory of turbulence. *Adv. Appl. Mech.* **1**, 171–199 (1948)
11. E.R. Benton, G.W. Platzman, A table of solutions of the one-dimensional Burgers equation. *Quart. Appl. Math.* **30**, 195–212 (1972)
12. W. Liao, An implicit fourth-order compact finite difference scheme for one-dimensional Burgers' equation. *Appl. Math. Comput.* **206**, 755–764 (2008)
13. E.N. Aksan, A. Ozdes, A numerical solution of Burgers' equation. *Appl. Math. Comput.* **156**, 395–402 (2004)
14. R. Jiwari, R.C. Mittal, K.K. Sharma, A numerical scheme based on weighted average differential quadrature method for the numerical solution of Burgers' equation. *Appl. Math. Comput.* **219**, 6680–6691 (2013)
15. R. Jiwari, Local radial basis function-finite difference based algorithms for singularly perturbed Burgers' model. *Math. Comput. Simul.* **198**, 106–126 (2022)
16. R. Jiwari, A hybrid numerical scheme for the numerical solution of the Burgers' equation. *Comput. Phys. Commun.* **188**, 59–67 (2015)
17. D. Li, C. Zhang, M. Ran, A linear finite difference scheme for generalized time fractional Burgers equation. *Appl. Math. Model.* **40**, 6069–6081 (2016)
18. T.S. El-Danaf, A.R. Hadhoud, Parametric spline functions for the solution of the one time fractional Burgers equation. *Appl. Math. Model.* **36**, 4557–4564 (2012)
19. A. Esen, O. Tasbozan, Numerical solution of time fractional Burgers equation by cubic B-spline finite elements. *Mediterr. J. Math.* **13**, 1325–1337 (2016)
20. S.E. Esipov, Coupled Burgers' equations: a model of polydisperse sedimentation. *Phys. Rev. E* **52**, 3711–3718 (1995)
21. S. Haq, M. Uddin, A meshfree interpolation method for the numerical solution of the coupled nonlinear partial differential equations. *Eng. Anal. Boundary Elem.* **33**, 399–409 (2009)
22. H. Jafari, S. Seifi, Solving a system of nonlinear fractional partial differential equations using homotopy analysis method. *Commun. Nonlinear Sci. Numer. Simul.* **14**, 1962–1969 (2009)
23. R.C. Mittal, G. Arora, Numerical solution of the coupled viscous Burgers' equation. *Commun. Nonlinear Sci. Numer. Simul.* **16**, 1304–1313 (2011)
24. R.K. Mohanty, W. Dai, F. Han, Compact operator method of accuracy two in time and four in space for the numerical solution of coupled viscous Burgers' equations. *Appl. Math. Comput.* **256**, 381–393 (2015)
25. M. Kumar, S. Pandit, A composite numerical scheme for the numerical simulation of coupled Burgers' equation. *Comput. Phys. Commun.* **185**, 809–817 (2014)
26. Y. Chen, H.L. An, Numerical solutions of coupled Burgers equations with time and space fractional derivatives. *Appl. Math. Comput.* **200**, 87–95 (2008)
27. J. Liu, G. Hou, Numerical solutions of space and time fractional coupled Burgers equations by generalized differential transform method. *Appl. Math. Comput.* **217**, 7001–7008 (2011)

28. A.K. Mittal, L.K. Balyan, Numerical solutions of time and space fractional coupled Burgers equations using time-space Chebyshev pseudospectral method. *Math. Meth. Appl. Sci.* **44**, 3127–3137 (2021)
29. M. Hussain, S. Haq, A. Ghafoor, I. Ali, Numerical solutions of time-fractional coupled viscous Burgers' equations using meshfree spectral method. *Comput. Appl. Math.* **39**, 1–21 (2020)
30. T.A. Sulaiman, M. Yavuz, H. Bulut, H.M. Baskonus, Investigation of the fractional coupled viscous Burgers' equation involving Mittag-Leffler kernel. *Physica A* **527**, 121126 (2019)
31. A.R. Hadhoud, H.M. Srivastava, A.A.M. Rageh, Non-polynomial B-spline and shifted Jacobi spectral collocation techniques to solve time-fractional nonlinear coupled Burgers' equations numerically. *Adv. Differ. Eq.* (2021). <https://doi.org/10.1186/s13662-021-03604-5>
32. R.C. Mittal, R.K. Jain, Numerical solutions of nonlinear Burgers' equation with modified cubic B-splines collocation method. *Appl. Math. Comput.* **218**, 7839–7855 (2012)
33. R. Chawla, K. Deswal, D. Kumar, A new numerical formulation for the generalized time-fractional Benjamin Bona Mohany Burgers' equation. *Int. J. Nonlinear Sci. Numer. Simul.* (2022). <https://doi.org/10.1515/ijnsns-2022-0209>

Publisher's Note Springer Nature remains neutral with regard to jurisdictional claims in published maps and institutional affiliations.

Springer Nature or its licensor (e.g. a society or other partner) holds exclusive rights to this article under a publishing agreement with the author(s) or other rightsholder(s); author self-archiving of the accepted manuscript version of this article is solely governed by the terms of such publishing agreement and applicable law.